Novel Shaped 8/16PSK Modulation with Improved Spectral Efficiency

Xiao Chen[1], Yu Zhou[1(✉)], Fan Gao[1], Xuesong Shao[1], Yue Li[1], Zhuowen Mu[1], and Hao Lu[2]

[1] State Grid Jiangsu Electric Power Co., Ltd., Marketing Service Center, Nanjing, China
lygnr@aliyun.com
[2] Hohai University, Nanjing 210098, China
luhao@hhu.edu.cn

Abstract. In this work, a precoder based on 8/16 phase shift keying (PSK) is devised and used to generate a novel shaped 8/16 PSK modulation combining precoding and continuous phase modulation (CPM). Then, two receivers based on Bahl-Cocke-Jelinek-Raviv (BCJR) algorithm and I-Q coherent detection are derived. Theoretical analysis and simulation are provided to show that the proposed modulation achieves higher spectral efficiency than the conventional CPM.

Keywords: Continuous phase modulation · Phase shift keying · Spectrum efficiency

1 Introduction

Recently, as a spectrally efficient modulation scheme, continuous phase modulation (CPM) has attracted great attention. Constant envelop and continuous phase allow for robustness against nonlinear distortion and high spectral efficiency. Due to these properties, CPM has been widely used in a number of fields such as satellite communications, deep-space communications and telemetry [1–3]. As one of the components in CPM, the mapper converts original binary bits to the data symbol belonging to alphabet of $\{\pm 1, \pm 3, \cdots, \pm(M-1)\}$, where M denotes the modulation order.

The design of alphabet has great impact on the signal spectral property and bit error rate (BER). To the best of our knowledge, few contributions have been made on the improvement to the CPM mapper. One approach uses precoder to replace mapper. Using this approach, an improved multi-h CPM to increase the minimum Euclidean distance of binary CPMs was proposed in [4] without considering bandwidth. Reference [5] focused on constraining the signal phase evolution of low modulation order CPM via precoding. Reference [6] described a form of CPM known as shaped binary phase shift keying (SBPSK) which is a constant envelope waveform modulation with a controlled phase trajectory based

Q. Guo et al. (Eds.): WiSATS 2021, LNICST 410, pp. 335–344, 2022.
https://doi.org/10.1007/978-3-030-93398-2_33

on BPSK. Motivated by SBPSK, [7] designed a ternary precoder $\{-1, 0, 1\}$ based on the phase state of offset quadrature phase-shift keying (OQPSK). It combined the precoder with CPM modulator to form a special case of CPM, SOQPSK, with higher spectral efficiency. However, none of them has studied higher order PSK.

In this paper, we propose a novel precoder based on 8/16PSK. The precoder converts the original binary sequence to the data symbol drawn from $\{0, \pm 1, \pm 2, \cdots, \pm(M/2-1), M/2\}$. The data symbol sequence is then modulated by a CPM modulator to generate shaped 8PSK and shaped 16PSK. Theoretical analysis shows that the proposed precoder can obtain narrower bandwidth at the cost of decreasing Euclidean distance between symbols. Simulation shows that the shaped 8PSK and shaped 16PSK can achieve up to 29% and 39% spectral efficiency gains over the conventional CPM with the same modulation order and modulation index, respectively.

2 System Model

The complex envelope of a CPM signal can be written as

$$s(t) = \sqrt{\frac{E_s}{T_s}} e^{j\phi(t)}, \tag{1}$$

where the phase of the signal $\phi(t)$ is given by

$$\phi(t) = 2\pi h \sum_i b_i q(t - iT_s). \tag{2}$$

E_s is the average energy per information symbol, T_s is the symbol interval, $h = r/p$ is the modulation index (r and p are relatively prime integers), the symbols $\{b_i\}$ are drawn from the alphabet $\mathbb{F} \triangleq \{\pm 1, \pm 3, \cdots, \pm(M-1)\}$ with modulation order $M = 2^k$, $q(t)$ is the phase-smoothing response with duration LT_s and area 1/2 and its derivative is the frequency pulse $g(t)$

$$g(t) = \begin{cases} \frac{1}{2LT_s} & 0 \le t \le LT_s \\ 0 & \text{else}, \end{cases} \tag{3}$$

L is the memory length. The modulation scheme is shown in Fig. 1(a), In each symbol duration, the mapper maps k bits of original binary bits directly into $\mathbb{F}$ to generate data symbol sequence. Then, the CPM modulator modulates the data symbol sequence using (1) and (2). Noted that in this letter, we constrain our research to 1REC modulation, namely, $L = 1$. Given that the modulation index is rational, (2) is further expressed as

$$\phi(t) = \underbrace{2\pi h b_n q(t - nT_s)}_{\theta(t)} + \underbrace{\pi h \sum_{i=0}^{n-1} b_i}_{\theta_{n-1}}, \tag{4}$$

where $nT_s \leq t < (n+1)T_s, n \in \mathbb{N}, \theta_n$ is the phase state which takes on p values and can be recursively defined as

$$\theta_n = [\theta_{n-1} + \pi h b_n]_{2\pi}, \tag{5}$$

where $[\cdot]_{2\pi}$ denotes the "modulo 2π" operator.

3 Proposed Precoder

Our aim is to improve the spectral efficiency of the conventional CPM. Instead of using the mapper, we propose a precoder based on 8/16PSK to convert the original binary bits to data symbols drawn from a different alphabet. The role of the precoder is to orient the phase of the CPM signal to make it behave like the phase of a 8/16PSK signal. We use 8PSK as an example to illustrate the rules of the precoder. Assuming $t = nT_s$, firstly, we map $k = 3$ bits of the original binary bits $\{a_{3(n-1)+1}, a_{3(n-1)+2}, a_{3n}\}$ to one state θ_n drawn from the 8PSK phase constellation $\{0, \pi/4, 2\pi/4, 3\pi/4, 4\pi/4, 5\pi/4, 6\pi/4, 7\pi/4\}$ by Gray code. Then, as shown in (5), $\pi h b_n$ depends on the phase rotation between the adjacent time interval. To disperse the spectral energy in a more uniform manner, we constrain the phase rotation within π. In other words, in 8PSK constellation, when the phase rotation between adjacent symbols surpasses π in the clockwise, it toggles to rotate in the counter-clockwise direction and vice versa. Therefore, $\theta_n - \theta_{n-1}$ belongs to $\{0, \pm 1/4\pi, \pm 2\pi/4, \pm 3\pi/4, \pi\}$ and we correspond $\pi h b_n$ to this set. Intuitively, we can set $h = 1/4$ to give the final symbol alphabet $\{0, \pm 1, \pm 2, \pm 3, 4\}$. We use a similar method for 16PSK. The operation to convert binary sequence $\{a_n\}$ to data symbols $\{b_n\}$ is summarized in Algorithm 1. Due to the precoding operation, in any given symbol interval, $\{b_n\}$ is drawn from the alphabet $\mathbb{F}' \triangleq \{0, \pm 1, \pm 2, \cdots, \pm(M/2-1), M/2\}$. Compared to the conventional mapper in CPM, the spacing of data symbols in the proposed precoder is smaller. Besides, the precoder can constrain the phase change within π. Thus, we can expect a decreased bandwidth.

We show the generation step of shaped 8/16PSK in Fig. 1 (b). The precoder converts the original binary bits $\{a_n\}$ to final data symbol sequence $\{b_n\}$ according to Algorithm 1. After passing through the CPM modulator using (1) and (2), we can obtain the shaped 8/16PSK.

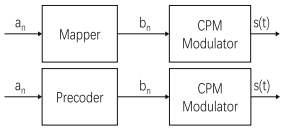

Fig. 1. Compared schemes. (a) Classical CPM, $b_n \in \{\pm 1, \pm 3, \cdots, \pm(M-1)\}$ and (b) Proposed Shaped 8/16PSK, $b_n \in \{0, \pm 1, \pm 2, \pm 3, 4\}$ for shaped 8PSK, $b_n \in \{0, \pm 1, \pm 2, \cdots, \pm 7, 8\}$ for shaped 16PSK.

Require: Original binary sequence $\{a_n\}$
Ensure: Final transmitted symbol sequence $\{b_n\}$
for all n **do**
  Convert $\{a_{3(n-1)+1}, a_{3(n-1)+2}, a_{3n}\}$ to decimal form de_n;
  $b_1 = de_1$;
  if n>1 **then**
    $b_n = de_n - de_{n-1}$;
  end if
  if $b_n \leq -M/2$ **then**
    $b_n = b_n + M$;
  else if $b_n \geq M/2$ **then**
    $b_n = b_n - M$;
  end if
end for

Algorithm 1: Shaped 8/16PSK Precoder

It is important to note that, in the following, we refer to the shaped 8/16PSK collectively as SMPSK due to the same precoding methods used. Where we need to distinguish, we will point out the different values of M. In addition, it is worth noting that to compare the difference between alphabets, the CPM in this letter is limited to 1REC CPM with the same modulation order M and modulation index h as SMPSK. In the following analysis, we denote it as MCPM.

In this letter, we use achievable spectral efficiency (ASE) to compare SMPSK with MCPM. ASE is one of the important metrics for communications. It represents the amount of information transmitted per unit of time and per unit of bandwidth. To compute ASE, we follow the approach in [8]

$$ASE = \frac{AIR}{BT_s} \tag{6}$$

where B is given by using the Carson's Rule measure, and achievable information rate (AIR) denotes the mutual information between channel input and channel output.

4 Receiver Design

Assuming that the channel is additive white Gaussian noise (AWGN) channel, the received signal is given by

$$y(t) = s(t) + w(t), \tag{7}$$

where $w(t)$ is a zero-mean white Gaussian process with two-sided power spectral density $N_0/2$. In this part, perfect frequency and time synchronization are assumed. Similar to SOQPSK, SMPSK can be constructed either by shaping the pulse of MPSK or connecting the proposed precoder with CPM modulator. Thus, we consider both the conventional MPSK I-Q coherent demodulator and optimal soft decision (i.e. BCJR) [9] could be deployed for reception.

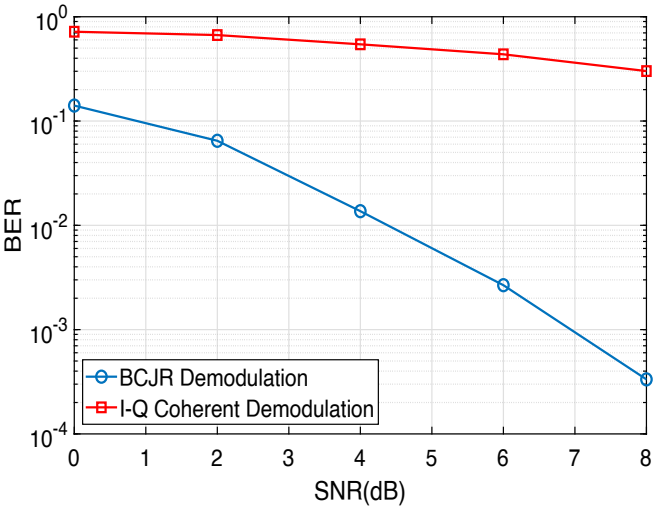

Fig. 2. BER comparison between two methods.

4.1 Receiver Based on BCJR

After the CPM modulation, the phase of SMPSK depends on the cumulative phase of previously transmitted symbols known as the phase memory. Therefore, we assume the SMPSK information sequence as finite and ergodic state Markov sequence, for which algorithms for maximum a posteriori symbol detection can be derived based on the BCJR algorithm. The transition between two states $c_{n-1} \rightarrow c_n$ corresponds to the transmitted symbol b_n.

Sampling the received signal $y(t)$ as $\boldsymbol{y} = (y_1, y_2, \cdots, y_N)$,

$$\hat{b}_n = \arg\max_{b_n \in \mathbb{F}'} p(b_n|\boldsymbol{y}), \tag{8}$$

where b_n denotes the symbol transmitted in the n^{th} time index. $\hat{b}_n$ is the symbol estimate in the n^{th} time index and $p(b_n|\boldsymbol{y})$ is the posteriori probability of the received signal. The transition between two states $c_{n-1} \rightarrow c_n$ corresponds to the transmitted symbol b_n. The conditional probability is given as,

$$p(b_n|\boldsymbol{y}) \propto \sum_{c_{n-1}} \alpha_{n-1}(c_{n-1})\beta(c_n)\gamma(c_n \rightarrow c_{n-1}, \boldsymbol{y})p(b_n). \tag{9}$$

The decision device chooses the symbol with the maximum a posteriori probability.

4.2 Receiver Based on I-Q Coherent Demodulation

As discussed in Sect. 3, each phase at symbol transition instants of SMPSK is drawn from the phase state in the MPSK constellation. Therefore, we adapt

the detection techniques for MPSK systems to the detection of SMPSK. The received signal is first demodulated by multiplying it with two coherent carriers $cos(2\pi f_c t)$ and $sin(2\pi f_c t)$. The resultant inphase and quadrature waveforms are lowpass filtered and sampled synchronously at $t = nT_s$. The phase θ_{n-1} is computed from the inphase and quadrature samples, and then decoded as one of the phases of MPSK. The receiver stores the decoded phase and then subtracts it from θ_n. Finally, the transmitted symbol is estimated as one of the values in $\mathbb{F}^{'}$. Figure 2 compares the two demodulation methods when $M = 8$ and $h = 1/4$. One sees that BCJR has better BER performance than I-Q coherent demodulation. This can be explained as follows. Firstly, BCJR pays attention to the distance between received signal and the possible transmitted signal in the whole time interval, while the I-Q coherent method only focuses on the distance in the symbol transition instants. Hence, the former can make full use of signal information. In addition, according to (5), if θ_n is incorrectly determined based on I-Q coherent demodulation, both b_n and b_{n+1} will be erroneously demodulated. In contrast, each symbol is independent in the BCJR demodulation. Hence, we use BCJR method to demodulate SMPSK in the following.

5 Performance Analysis

We derive the AIR of each modulation and then use it to compute the ASE. We consider AIR by modelling the SMPSK as finite and ergodic Markov chain. AIR denotes the mutual information between channel input and channel output over all possible input distributions $I(X, Y)$ as

$$\begin{aligned} I(X,Y) &= \lim_{N\to\infty} \frac{1}{N} I(X_1^N, Y_1^N) \\ &= \lim_{N\to\infty} [\frac{1}{N} H(X_1^N) - \frac{1}{N} H(X_1^N | Y_1^N)] \end{aligned} \tag{10}$$

where X_1^N is the transmitted data symbol sequence, and Y_1^N is the corresponding vector of the AWGN channel outputs. Then, we have

$$\frac{1}{N} H(X_1^N) = lbM, \tag{11}$$

and

$$\begin{aligned} \frac{1}{N} H(X_1^N | Y_1^N) &= \frac{1}{N} H(C_0^N | Y_1^N) \\ &= \frac{1}{N} \sum_{i=1}^{N} H(C_i | C_0^{i-1}, Y_1^N). \end{aligned} \tag{12}$$

Since C_0^{i-1} is already known and C_i is independent of C_0^{i-2},

$$\begin{aligned} &H(C_i | C_0^{i-1}, Y_1^N) \\ &= E_{p(C_{i-1}, Y_1^N)}(H(C_i | C_{i-1} = c_{i-1}, Y_1^N = y_1^N)) \\ &= E_{p(C_{i-1}, Y_1^N)} \\ &* \{E_{p(C_i | C_{i-1} = c_{i-1}, Y_1^N = y_1^N)}(lb(p(C_i | C_{i-1} = c_{i-1}, Y_1^N))\}, \end{aligned} \tag{13}$$

which can be computed from the BCJR algorithm.

We do not have a closed-form expression of AIR since BCJR algorithm is a simulation-based method. Nevertheless, state transition probability $p(C_i|C_{i-1} = c_{i-1}, Y_1^N)$ depends on the minimum squared Euclidean distance between different signals. Increasing the minimum Euclidean distance between different signals gives higher AIR. The minimum squared Euclidean distance d^2_{min} of 1REC CPM is [10],

$$\begin{aligned} d^2_{min} &= 2lbM[1 - sinc(\gamma h)] \\ &= 2lbM[1 - sinc(\gamma * (2/M))] \end{aligned} \tag{14}$$

where $\gamma = b_i - b_i^{'}$ denotes the error event between two symbols. Using the smallest value of γ, $\gamma = 2$ for MCPM and $\gamma = 1$ for SMPSK. Further, it can be concluded that the minimum squared Euclidean distance is $d^2_{min} = 2lbM[1 - sinc(2/(M/2))]$ for MCPM and $d^{'2}_{min} = 2lbM[1 - sinc(1/(M/2))]$ for SMPSK.

We can see that the minimum squared Euclidean distance of proposed SMPSK is smaller and therefore it yields lower AIR than MCPM.

Secondly, for the denominator in (6), assuming that the same symbol interval T_s for both modulation schemes, we focus on the bandwidth B. Conventional research tends to deploy 99% power bandwidth. Unfortunately, this makes theoretical comparison of signals with different symbol alphabets difficult. The problem can be solved by using the Carson's Rule bandwidth measure, which decreases the complexity and still provides good bandwidth estimation for CPM. Denote the unmodulated signal as $m(t) \equiv \sum_i b_i g(t - iT_s)$. The definition of Carson's Rule bandwidth is [8]

$$B = 2h\sqrt{P_m} + 2f_m, \tag{15}$$

where P_m is the power of $m(t)$ and f_m is the one-sided effective bandwidth of $m(t)$. $f_m = P_m/(2S_m(0))$, where $S_m(f)$ is the power spectral density of $m(t)$. Since f_m can be derived from P_m, we only discuss P_m. According to [8], the power of the unmodulated MCPM signal is

$$P_m = \frac{M^2 - 1}{3T_s} \int_0^{T_s} g^2(t)dt. \tag{16}$$

The power of the unmodulated SMPSK signal is,

$$\begin{aligned} P_m^{'} &= (\frac{(\frac{M}{2} - 1)(M - 1)}{6T_s} + \frac{M}{4T_s}) \int_0^{T_s} g^2(t)dt \\ &= \frac{M^2 + 2}{12T_s} \int_0^{T_s} g^2(t)dt. \end{aligned} \tag{17}$$

Comparing (16) and (17), one sees that the final bandwidth occupied by SMPSK is narrower than that by MCPM as

$$\begin{aligned}\Delta B &= 2h\sqrt{P_m} + 2f_m - (2h\sqrt{P_m^{'}} + 2f_m^{'}) \\ &= 2h\sqrt{P_m} + \frac{6T_sP_m}{M^2-1} - (2h\sqrt{P_m^{'}} + \frac{24T_sP_m^{'}}{M^2+2}) \\ &= \frac{2}{MT_s}\cdot(\sqrt{\frac{M^2-1}{3}} - \sqrt{\frac{M^2+2}{12}})\end{aligned} \tag{18}$$

where $f_m^{'}$ denotes the one-sided effective bandwidth of SMPSK. When $M > 1$, SMPSK requires less spectrum resources than MCPM.

These results show that the modulation providing higher information rate is not necessarily the one providing narrower bandwidth. Additionally, AIR depends on the simulation-based BCJR algorithm. Therefore, it is difficult to derive a closed-form result on which modulation method is more spectrally efficient.

6 Numerical Results and Discussion

In this section, we compare the two modulation schemes by simulation when AWGN channel is assumed. We set symbol number is 500 and $T_s = 40\,\mu s$. We use a Monte Carlo simulation to estimate the AIR and ASE of these modulations. Table 1 gives the occupied bandwidth of SMPSK and MCPM according to (15). Figure 3 shows how the AIR varies with SNR when different modulations are considered. First of all, it is natural that higher order modulation with higher transmission rate could achieve higher AIR for high SNRs. Second, for low SNRs, the larger minimum squared Euclidean distance is, the less sensitive it will be to noise, and therefore the higher the resulting AIR will be. It is clear that MCPM and low order modulation with larger minimum Euclidean distance can achieve higher AIR for low SNRs.

Table 1. Occupied bandwidth for different schemes.

Modulation scheme	Occupied bandwidth
S8PSK	$1.586/T_s$
8CPM 1REC, $h = 1/4$	$2.146/T_s$
S16PSK	$1.579/T_s$
16CPM 1REC, $h = 1/8$	$2.152/T_s$

On the other hand, Fig. 4 shows the ASE for the same modulations as in Fig. 3. These results show that the modulation providing the higher AIR is not

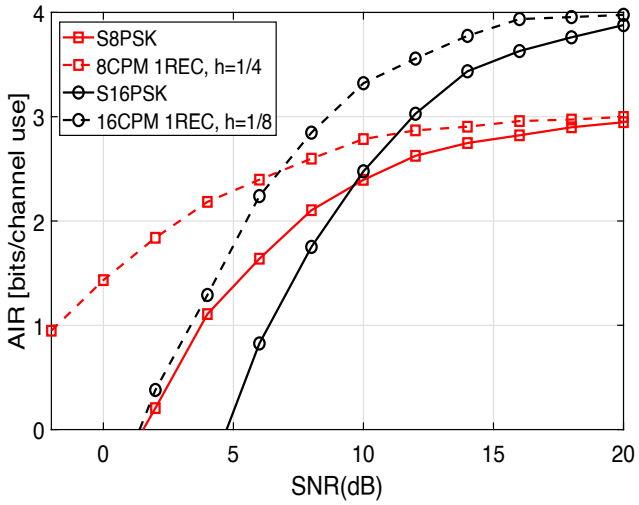

Fig. 3. Achievable information rate for different schemes.

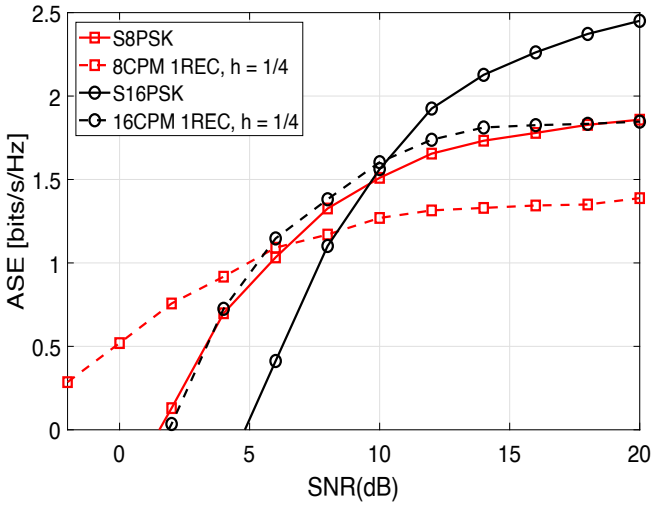

Fig. 4. Achievable spectal efficiency for different schemes.

that with higher ASE. Specifically, SMPSK outperforms MCPM by 29% to 39% in terms of spectral efficiency, when $M = 8$ and $M = 16$ at SNR is 20dB, respectively. This benefits from its precoder, which requires less bandwidth. Therefore, when the ASE is the key performance measure, we can trade degradation in AIR for improvement in ASE. We will consider SMPSK's unsatisfactory performance at low SNR in future work.

7 Conclusion

In this letter, we have proposed a novel precoder based on 8/16PSK. We connect the precoder with CPM modulator to generate a novel CPM modulation scheme shaped 8/16PSK. The analysis and simulation show that the proposed modulation scheme can obtain higher spectral efficiency than conventional CPM.

Acknowledgements. This work was supported by Research on Performance Evaluation and Optimization Technology of Local IOT for Client-side Metering Equipment under grant No. 5700-202118203A-0-0-00.

References

1. Bing, L., Aulin, T., Bai, B., Zhang, H.: Design and performance analysis of multiuser CPM with single user detection. IEEE Trans. Wirel. Commun. **15**(6), 4032–4044 (2016)
2. Wattamwar, R.R., Handore, P.S.: Comparison of bit error rate evaluation for SISO and MIMO system by CPM modulation technique using Matlab. In: 2018 International Conference On Advances in Communication and Computing Technology (ICACCT), pp. 269–272, February 2018
3. Xue, R., Yu, H., Cheng, Q.: Adaptive coded modulation based on continuous phase modulation for inter-satellite links of global navigation satellite systems. IEEE Access **6**, 20652–20662 (2018). https://doi.org/10.1109/ACCESS.2018.2825255
4. Fonseka, J.P.: Nonlinear continuous phase frequency shift keying. IEEE Trans. Commun. **39**(10), 1473–1481 (1991)
5. Messai, M., Piemontese, A., Colavolpe, G., Amis, K., Guilloud, F.: Binary CPMs with improved spectral efficiency. IEEE Commun. Lett. **20**(1), 85–88 (2016)
6. Dapper, M.J., Hill, T.J.: SBPSK: a robust bandwidth-efficient modulation for hard-limited channels. In: IEEE Military Communications Conference, MILCOM 1984, vol. 3, pp. 458–463, October 1984
7. DIS Agency: Department of Defense interface standard, interoperability standard for single-access 5-kHz and 25-kHz UHF satellite communications channels. Department of Defense, March 1999
8. Kuo, C.-H., Chugg, K.M.: On the bandwidth efficiency of CPM signals. In: IEEE MILCOM 2004, Military Communications Conference, vol. 1, pp. 218–224, October 2004
9. Bahl, L.R., Cocke, J., Jelinek, F., Raviv, J.: Optimal decoding of linear codes for minimizing symbol error rate (corresp.). IEEE Trans. Inf. Theory **20**(2), 284–287 (2003)
10. Ekanayake, N., Liyanapathirana, R.: On the exact formula for the minimum squared Euclidean distance of CPFSK. IEEE Trans. Commun. **42**(11), 2917–2918 (1994)